

## Extreme Ultraviolet Radiation Transport in Laser-Irradiated High-Z Metal Foils

J. Mizui, N. Yamaguchi, and S. Takagi<sup>(a)</sup>

*Institute of Plasma Physics, Nagoya University, Nagoya 464, Japan*

and

K. Nishihara

*Institute of Laser Engineering, Osaka University, Suita 565, Japan*

(Received 18 March 1981)

Spatially resolved extreme ultraviolet spectra were measured from the rear side of gold foils irradiated with 1.05- $\mu\text{m}$  wavelength, 100-ps pulses at intensities of  $3 \times 10^{14}$  W/cm<sup>2</sup>. In the energy range of 0.1 to 1.0 keV the radiation intensity decayed exponentially with foil thickness up to 1  $\mu\text{m}$  but remained almost constant over the range of 1 to 6  $\mu\text{m}$ . These results indicate that radiation heat conduction plays an important role in high-Z plasma energy transport. Ablation by the radiation heat flux is briefly discussed.

PACS numbers: 52.50.Jm, 52.25.Ps, 52.25.Fi

Emission and reabsorption of extreme ultraviolet (XUV) radiation play an important role in high-Z plasma energy transport.<sup>1</sup> Conversion efficiencies from laser energy to XUV radiation energy have been measured with multichannel x-ray diodes and range from 15% to 2.3% for laser intensities of  $10^{14}$  to  $10^{16}$  W/cm<sup>2</sup> and gold targets.<sup>2</sup> The spectrum has been shown to be Planckian with color temperatures ranging from 66 to 134 eV. When the outward radiation flux is as large as observed and a target plasma is optically thick to the radiation, inward radiation flux heats a plasma inside the target. In this Letter we report on the first direct measurement of the transport of XUV radiation through high-Z (gold) and low-Z (aluminum) foils. We also estimate the front- and rear-side plasma temperatures for the gold foils.

The experimental setup is shown in Fig. 1. The experiments were performed on the HALNA Nd:phosphate-glass laser system with an output energy of 7 to 15 J in a pulse of 100 ps full width at half maximum. The laser output was focused to a 200- $\mu\text{m}$ -diam spot with an  $f/1.33$  aspheric lens, giving an intensity of  $3 \times 10^{14}$  W/cm<sup>2</sup>. Targets were 5-mm-wide foils of gold or aluminum with thicknesses from 0.5 to 10  $\mu\text{m}$ . For the Au foils, the support resin was removed in acetone and irradiation was on the initially uncoated surface. The spectrum was measured using a grazing-incidence ( $88^\circ$ ) spectrograph with a 2-m-radius gold-coated concave grating. Spatial resolution was achieved by inserting a 100- $\mu\text{m}$ -wide slit between the 10- $\mu\text{m}$ -wide entrance slit and the grating.<sup>3</sup> Single shot spectra were recorded on Kodak SC-7 film. Wavelength and film calibration were performed in a separate experiment.

XUV spectra from the laser-irradiated plasma

were recorded with the laser incident at  $20^\circ$  to the target normal, as shown by the solid line in Fig. 1. Rear-side spectra were recorded with the same incident angle as shown by the dashed line. Evidence for radiation transport through the target was obtained by comparing these two spectra for different foil thicknesses. The laser-irradiated plasma spectrum was essentially independent of the foil thickness and, for the gold targets, consisted of many closely spaced lines in the wavelength ranges of 25–35 and 45–55  $\text{\AA}$  as shown in Fig. 2(a). The latter group has also been observed in tokamak plasmas<sup>4</sup> and comes from highly ionized Au<sup>+16</sup> to Au<sup>+24</sup>. This plasma can be considered as a source of radiation which heats the target interior. The rear spectrum also contained these two groups of lines, but of somewhat weaker intensity, and two lines of C<sup>+4</sup> and C<sup>+5</sup> from residual traces of the foil support resin

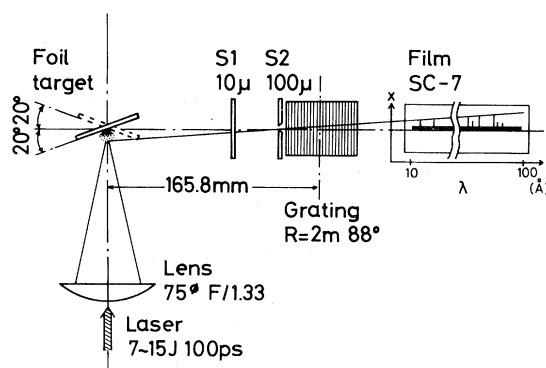


FIG. 1. Experimental setup. S1 is a slit for wavelength dispersion and S2 is a slit for spatial resolution. The XUV spectrum from the laser-side plasma is obtained with the target setting shown with the solid line and that from the rear-side one with the dashed line.

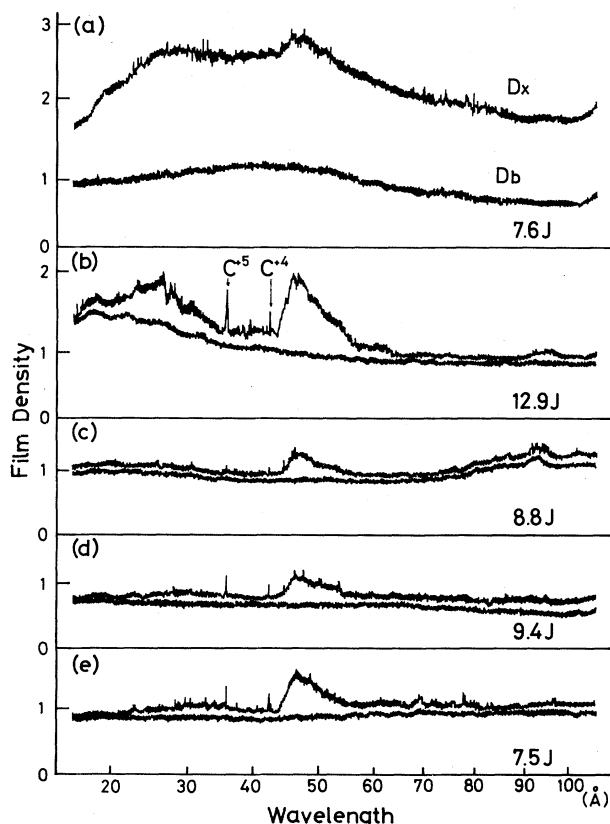


FIG. 2. Densitometer traces of XUV spectra from Au-foil targets. (a) The radiation spectrum from the laser-side plasma. (b)–(e) Radiation spectra from the rear-side plasmas with 0.5- $\mu\text{m}$  Au-foil thickness for (b), 1  $\mu\text{m}$  for (c), 3  $\mu\text{m}$  for (d), and 6  $\mu\text{m}$  for (e).  $D_x$  is the film density of the diffracted radiation and  $D_b$  is that of the stray-background light.

as shown in Figs. 2(b)–2(e). If the initially resin-coated surface was irradiated with the laser, these carbon lines were not observed from the rear-side plasma, indicating that the target is optically thick to the XUV radiation. The observation of the highly ionized gold and carbon lines from the rear surface therefore indicates a high-temperature rear-surface plasma. For the gold foils rear-surface spectra were observed for thicknesses up to 6  $\mu\text{m}$  but not for 10- $\mu\text{m}$ -thick foils. On the other hand, for Al foil targets comparable spectra were only recorded for 1.5- $\mu\text{m}$ -thick foils, and not for 3- $\mu\text{m}$ -thick targets.

The XUV radiation intensity from the rear surface is plotted as a function of foil thickness in Fig. 3. The intensities are measured at 52.4  $\text{\AA}$  (Al XI,  $2p^2P-3d^2D$ ) and 50.0  $\text{\AA}$  (continuum) for aluminum and at 47  $\text{\AA}$  (many closely spaced lines) for gold. For aluminum [Fig. 3(a)] the intensity

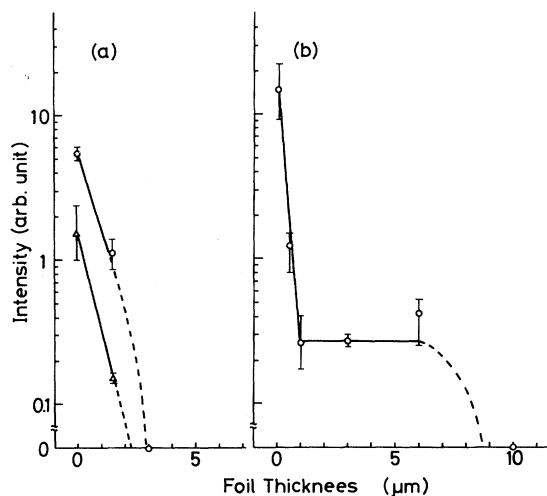


FIG. 3. Radiation intensities as functions of the foil thickness. (a) Open circles show the data for 52.4- $\text{\AA}$  (Al XI,  $2p^2P-3d^2D$ ) and open triangles the data for 50.0- $\text{\AA}$  (continuum) radiation from the aluminum. (b) The data for 47- $\text{\AA}$  radiation from the gold. The data for the 0- $\mu\text{m}$  foil thickness are taken from the radiation of the laser-side plasma.

decays exponentially with a scale length of 0.69 to 0.80  $\mu\text{m}$  and goes to zero at 3  $\mu\text{m}$ . Here, the zero-intensity point indicates that the diffracted radiation cannot be distinguished above the stray-background light in our system. For gold the intensity also decays exponentially initially with a scale length of 0.20  $\mu\text{m}$ , but for thickness from 1 to 6  $\mu\text{m}$  the intensity remains almost constant [Fig. 3(b)]. The exponential decay scale lengths are several times larger than the absorption lengths for the un-ionized target materials,<sup>5,6</sup> but are consistent with the absorption lengths in highly ionized material.<sup>6,7</sup> Suprathermal electron heating is also another candidate to explain the exponential part of the decay curves.

Before discussing the energy transport processes it is necessary to estimate the front- and rear-side plasma temperature for our experiment. To estimate the front surface temperature the Au target was irradiated with two laser pulses at normal incidence with a separation of 8 ns. After the first pulse the plasma expands normal to the target surface and the second pulse then produces a second XUV-emitting region. From the separation of the two emission regions of 250–350  $\mu\text{m}$  as shown in Fig. 4 and the pulse separation we estimate the expansion velocity to be  $(3.1-4.4) \times 10^6$  cm/s. Assuming that this velocity is of the order of the sound velocity, we get a product of average ion charge,  $\langle z \rangle$ , and electron tempera-

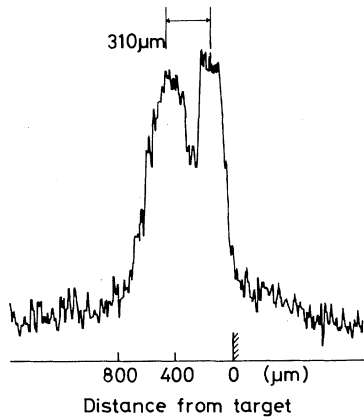


FIG. 4. Spatial distribution of XUV radiation at the wavelength of 47 Å for 10- $\mu\text{m}$ -thick Au foil. Two laser pulses, whose interval is 8 ns, are incident on the target from the left in this figure.

ture,  $T_e$ , of 1.2 to 2.4 keV. For local thermodynamic equilibrium (LTE) we can then estimate that  $\langle z \rangle \simeq 14$  and  $T_e \simeq 130$  eV. For the rear-side temperature we use the intensity ratio of the C<sup>+5</sup> and C<sup>+4</sup> lines. For 0.5- $\mu\text{m}$ -thick gold foils this ratio was  $2.2 \pm 0.2$  and for 1.0- to 6.0- $\mu\text{m}$ -thick foils it was  $1.1 \pm 0.3$ . For LTE and an ion density equal to solid density, we estimate temperatures of  $125 \pm 10$  eV for 0.5- $\mu\text{m}$ -thick foils and  $100 \pm 10$  eV for 1- to 6- $\mu\text{m}$ -thick foils. For coronal equilibrium these temperatures become  $90 \pm 5$  eV and  $80 \pm 5$  eV, respectively. From these estimates we can conclude that there is a plateau in the rear-side temperature of many tens of eV which is almost constant for Au foil thickness from 1 to 6  $\mu\text{m}$ .

We can consider suprathreshold electron and radiation as candidates for anomalous energy transport through the gold foil. According to Max and Estabrook,<sup>8</sup> with the laser intensity of  $3 \times 10^{14}$  W/cm<sup>2</sup>,  $\langle z \rangle$  of 14, and the cold-electron temperature of 130 eV, the hot-electron temperature and its range are estimated to be 3.2 keV and 1.8  $\mu\text{m}$ , respectively. The range is smaller than the foil thickness of 6  $\mu\text{m}$ . The radiation from the rear-surface plasma of the gold was observed even in the case of the thicker foils compared with the aluminum. To explain the results, both energy and number density of hot electrons in the gold are then required to be extremely greater than those in the aluminum, since the range in a high- $Z$  plasma is shorter than that in a low- $Z$  plasma. Although heating through the foil by hot electrons cannot be ruled out, it is difficult to ex-

plain the data only in terms of suprathreshold electron heating.

Under the assumption that the radiation is blackbody with a color temperature of the same order as the plasma temperature of 130 eV, and using a diffusion approximation with the Rosseland bound-free mean free path in solid density,<sup>9</sup> we can estimate the ratio of radiation to thermal electron heat flux to be greater than 100. In a high- $Z$  gold plasma the radiations are dominantly emitted by bound-bound transitions, as shown in Fig. 2. Since we do not yet have precise knowledge of the absorption mean free path for the many closely spaced lines, in this Letter we use the Rosseland bound-free mean free path instead. The mean free path with bound-bound absorption has been calculated to be shorter only by a factor of 3 than that without it at any particular temperature.<sup>10</sup> Therefore, although our estimate of the path has an error, the radiation heat flux can be much greater than the thermal electron heat flux. Under these conditions ablation of the plasma by radiation heat flux can occur in gold,<sup>11</sup> as has been observed in relativistic electron beam experiments.<sup>12</sup> The ablation plays the role of a piston and drives a shock wave ahead of itself. We now estimate the radiation heat flux by assuming that the inward radiation flux supports the ablation, and that the rear-side plasma is heated only by the shock wave. If we assume steady ablation for simplicity, the inward radiation heat flux,  $Q_r$ , required at the Chapman-Jouguet point to maintain the ablation can be approximately given as

$$Q_r \cong \left[ \frac{3}{2} n_2 (z_2 + 1) T_2 + \frac{1}{2} m_i n_2 c_2^2 + p_2 \right] c_2 = 3 p_2 c_2, \quad (1)$$

if  $n_1 \gg n_2$ , where  $n$ ,  $p$ , and  $c$  are, respectively, the ion density, the pressure, and the sound velocity, and the subscripts 1 and 2 indicate the variables in the shock-compressed region and at the Chapman-Jouguet point, respectively. For a strong shock,  $n_1 \sim 4n_0$  and  $v_s \sim 4c_1/\sqrt{3}$ , and if  $n_1 \gg n_2$ ,  $p_2 \sim p_1/2$ , where  $n_0$  and  $v_s$  are the initial target density and the shock front velocity, respectively. Using those relations, we get

$$Q_r \lesssim \frac{9}{8} m_i n_0 v_s^2 c_2, \quad (2)$$

which can give the maximum value of the inward radiation heat flux. For  $c_2$ , we use the sound velocity obtained from the measurement of the laser-irradiated plasma expansion velocity. The shock front velocity is estimated by use of the measured rear-surface temperature and the

strong shock relation. The radiation heat flux is then calculated from Eq. (2) to be  $1.0 \times 10^{14}$  W/cm<sup>2</sup> and the conversion efficiency from laser to XUV radiation is 33%. Also the width of the ablation front is estimated to be 1  $\mu$ m.<sup>11</sup> Using the relation  $Q_r = (c\lambda_{bf}/3)(\partial U_r/\partial x)$ , where  $\lambda_{bf}$  and  $U_r$  are the Rosseland mean free path for bound-free absorption and the radiation energy density, respectively, we estimate the color temperature as 150 eV. These values can be overestimated since we have assumed that the rear-side plasma is heated only by the shock wave. The temperature of the rear-surface plasma is higher than that heated by the shock wave, because of additional heating by suprathermal electrons, and also because the hot region of the ablation front reaches the rear surface after the shock wave. This model has, however, an advantage to explain the almost constant temperature of the rear surface for thickness from 1 to 6  $\mu$ m, since the shock-heated plasmas have the same temperature under the constant heat flux. It cannot be assumed that the shock front reaches the rear surface of gold foils thicker than 6  $\mu$ m within the duration of the heat flux. A more definitive explanation of the plateau of the radiation intensity calls for further measurements of, for example, the duration time of the heat flux and the break-out time on the rear of the foil.

To summarize, spatially resolved XUV spectra from the rear side of laser-irradiated aluminum- or gold-foil targets have been observed in the energy range of 0.1 to 1.0 keV. For aluminum the radiation intensity decays to zero at 3  $\mu$ m. For gold the radiation intensity also decays exponentially up to 1  $\mu$ m, but from 1 to 6  $\mu$ m it remains constant. In the latter case the rear-side temperature is higher than several tens of electronvolts for foils from 1 to 6  $\mu$ m thick. These re-

sults and the simple theoretical calculation indicate that radiation heat conduction plays an important role in the high- $Z$  plasma energy transport. The possibility of ablation by radiation heat flux is also discussed.

We would like to thank Professor C. Yamanaka, Professor S. Hayakawa, Professor J. Fujita, and Dr. A. Raven for valuable discussions and Professor M. Otuka for the guidance on the design of the spectrograph. Thanks are also due to Mr. H. Yonezu for his technical assistance.

<sup>(a)</sup>Also at Faculty of Engineering, Doshisha University, Kyoto 602, Japan.

<sup>1</sup>J. Mizui *et al.*, Phys. Rev. Lett. **39**, 619 (1977).

<sup>2</sup>P. D. Rockett, W. Priedhorsky, and D. Giovanielli, Los Alamos Scientific Laboratory Report No. LA-UR-80-2442, to be published; M. D. Rosen *et al.*, Phys. Fluids **22**, 2020 (1979).

<sup>3</sup>F. E. Irons and N. J. Peacock, J. Phys. E **6**, 857 (1973).

<sup>4</sup>S. Kasai *et al.*, Nucl. Fusion **19**, 195 (1979); B. M. Johnson *et al.*, Phys. Lett. **70A**, 320 (1979).

<sup>5</sup>B. L. Henke and E. S. Ebinu, University of Hawaii Interim Report, Grant No. AFOSR 72-2174 (unpublished).

<sup>6</sup>R. F. Reilman and S. T. Manson, Astrophys. J., Suppl. Ser. **40**, 815 (1979).

<sup>7</sup>N. Yamaguchi, J. Phys. Soc. Jpn. **47**, 299 (1979); E. A. McLean *et al.*, Phys. Rev. Lett. **45**, 1246 (1980).

<sup>8</sup>C. Max and K. Estabrook, Comments Plasma Phys. Controlled Fusion **5**, 239 (1980).

<sup>9</sup>Ya. B. Zel'dovich and Yu. P. Raizer, *Physics of Shock Waves and High-Temperature Hydrodynamic Phenomena* (Academic, New York, 1966).

<sup>10</sup>E. Nardi and Z. Zinamon, Phys. Rev. A **20**, 1197 (1979).

<sup>11</sup>K. Nozaki and K. Nishihara, J. Phys. Soc. Jpn. **48**, 993 (1980).

<sup>12</sup>S. L. Bogolyubshi *et al.*, Pis'ma Zh. Eksp. Teor. Fiz. **24**, 202 (1976) [JETP Lett. **24**, 178 (1976)].